Journal of Membrane Science 450 (2014) 299–307

Contents lists available at ScienceDirect

Journal of Membrane Science

journal homepage: www.elsevier.com/locate/memsci

Pd-based binary and ternary alloy membranes: Morphological and perm-selective characterization in the presence of H_2S

Fernando Braun [a], Ana M. Tarditi [a], James B. Miller [b,c], Laura M. Cornaglia [a,*]

[a] Instituto de Investigaciones en Catálisis y Petroquímica (FIQ, UNL-CONICET), Santiago del Estero 2829, 3000 Santa Fe, Argentina
[b] Department of Chemical Engineering, Carnegie Mellon University, Pittsburgh, PA, United States
[c] National Energy Technology Laboratory, US Department of Energy, Pittsburgh, PA, United States

ARTICLE INFO

Article history:
Received 23 May 2013
Received in revised form
11 September 2013
Accepted 14 September 2013
Available online 20 September 2013

Keywords:
PdAgAu alloy
Sulfur tolerance
Ternary alloy
Hydrogen separation membrane

ABSTRACT

Pd, $Pd_{90}Ag_{10}$, $Pd_{91}Au_9$, $Pd_{78}Ag_9Au_{13}$ and $Pd_{75}Ag_{16}Au_9$ alloy membranes were prepared on vacuum-assisted ZrO_2-modified porous stainless steel supports by sequential electroless deposition. The membranes were evaluated for permeability in pure H_2 and in an H_2S/H_2 mixture. The membranes displayed a range of permeabilities in pure H_2: $Pd_{90}Ag_{10} > Pd_{78}Ag_9Au_{13} > Pd \sim Pd_{75}Ag_{16}Au_9 > Pd_{91}Au_9$. On exposure to 100 ppm H_2S/H_2 at 673 K for 24 h, all membranes lost a significant fraction of their H_2 permeabilities: Pd (lost the largest fraction, 85%) > $Pd_{90}Ag_{10} > Pd_{75}Ag_{16}Au_9 > Pd_{78}Ag_9Au_{13} > Pd_{91}Au_9$ (60%). When H_2S was removed, the membranes recovered the lost permeability to different extents. The $Pd_{91}Au_9$ and $Pd_{78}Ag_9Au_{13}$ membranes displayed the highest fractional recovery of initial H_2 permeability (~80%). But, with its higher initial pure H_2 permeability, $Pd_{78}Ag_9Au_{13}$ had the highest absolute H_2 permeability after recovery. The microstructure, morphology and bulk composition of H_2S-exposed samples were characterized by X-ray diffraction (XRD), scanning electron microscopy (SEM) and energy-dispersive X-ray spectroscopy (EDS). XRD revealed the presence of a bulk Pd_4S phase on both Pd and $Pd_{90}Ag_{10}$, the membranes that recovered the least H_2 relative flux after their exposure to H_2S. In contrast, bulk sulfides did not form on $Pd_{91}Au_9$ or on PdAgAu ternary alloys. In agreement with the XRD results, EDS did not detect sulfur in the bulk of $Pd_{91}Au_9$ or in either of the ternary alloy samples. Our results show that the addition of Au to the high-permeability PdAg binary membrane results in a PdAgAu ternary membrane that minimizes the permanent H_2 flux loss associated with H_2S exposure by preventing the formation of thick stable sulfides.

1. Introduction

Hydrogen can be used for electricity generation in fuel cells without greenhouse gas emission. To avoid deactivation of catalytic surfaces in low-temperature PEM fuel cells, H_2 must be nearly free of trace impurities, including CO and H_2S. H_2 production from fossil-derived syngas can require multiple stages of purification to completely remove these minor components. Dense Pd membranes have received considerable attention for H_2 purification application. Molecular H_2 dissociates on a Pd catalytic surface to form H atoms, which readily diffuse through Pd bulk. Recombination of the atoms on the opposite surface of the membrane to reform H_2 molecules completes a sequence that delivers near perfect separation selectivity [1–3]. In practical implementations, Pd membranes become brittle in the presence of H_2. Furthermore, H_2S, a common component of fossil-derived syngas, can react with the Pd surface to form a Pd_4S sulfide scale, which has only a fraction of the permeability of pure Pd and which can cause mechanical failure [4,5].

Alloying Pd with one or more components has been employed to improve both its structural properties and its response to H_2S. Some components, such as Ag, increase the H_2 permeability of Pd. The reasons for the permeability increase are complex, but can be thought of in terms of increased H atom solubility and diffusivity that accompanies the expansion of the Pd lattice by insertion of the relatively large Ag atom [6]. However, PdAg, like pure Pd, is well known to form bulk sulfides in the presence of H_2S over a wide range of exposure conditions [7,8].

Other components have been alloyed with Pd specifically for the improvement of the H_2S response [7,9–14]. PdCu alloys have been thoroughly studied for sulfur tolerance; their responses to H_2S exposure are complex functions of alloy composition and exposure conditions. At moderate temperatures ($\leq$ 723 K), low Cu content alloys ($\leq$ 30 at%) form low permeability bulk corrosion layers [12,15,16], whereas high Cu content alloys experience

* Corresponding author. Tel.: +54 342 4536861.
E-mail addresses: lmcornag@fiq.unl.edu.ar, lcornaglia2002@yahoo.com (L.M. Cornaglia).

0376-7388/$ - see front matter © 2013 Elsevier B.V. All rights reserved.
http://dx.doi.org/10.1016/j.memsci.2013.09.026

complete inhibition of hydrogen transport, likely due to a combination of surface sulfide formation and site blocking by adsorbed H_2S [15,17]. At higher temperatures (> 900 K), PdCu is indifferent to the presence of H_2S [12]; unfortunately, a cost-effective implementation of membrane technology requires that the separation be performed at significantly lower temperatures.

Au, an alloy component studied in this work, has also been used to improve the H_2S response of Pd [9,13,14]. Direct comparisons of PdAu and PdCu are rare; at least at high alloying rates (> 20% minor component), Au appears to be more effective than Cu [8]. At lower concentrations, i.e., $Pd_{95}Au_5$, Au prevents bulk sulfide formation and partially preserves permeability when exposed to H_2S/H_2 mixtures [13]. However, when the H_2S exposure takes place in a WGS mixture (CO_2, CO, H_2O) background, bulk sulfide formation occurs [14] even at mild conditions (673 K and 20 ppm (mg kg^{-1}) H_2S).

Ternary Pd alloys have been considered for their potential to improve both permeability and H_2S response [18–22]. In general, components that increase pure H_2 permeability in binary alloys with Pd, Ag for example, also improve the permeability of a ternary alloy. Moreover, few reports of the H_2S response of ternary membranes have been published [20–22], mainly on self-supported membranes deposited by magnetron sputtering. We previously reported that $Pd_{83}Ag_2Au_{15}$ and $Pd_{74}Ag_{14}Au_{12}$ alloy membranes, both synthesized by electroless plating, do not experience bulk sulfide corrosion, even when exposed to 1000 ppm H_2S/H_2 [20]. $Pd_{87-89}Au_{7-5}Pt_6$ has been observed to display better H_2S response than $Pd_{88}Au_{12}$ in WGS backgrounds [22]. Within a series of ~$Pd_{75}Ag_{20}X_5$ (X=Au, Mo, Cu, Y) alloys prepared by sputter deposition methods, the Au-containing ternary exhibited both the smallest fractional flux loss upon exposure to H_2S and the lowest post-exposure surface S content [21].

With the aim of combining the H_2S tolerance of the PdAu binary with the high permeability of the PdAg binary, we prepared ternary PdAgAu alloys and reference PdAu and PdAg binaries by sequential electroless plating. We characterized the membranes for the inhibition of hydrogen transport by H_2S (100 ppm H_2S/H_2 at 673 K) and flux recovery in a pure H_2 atmosphere. Unlike Pd and $Pd_{90}Ag_{10}$, $Pd_{91}Au_9$ and the ternary alloys do not react with H_2S to form bulk sulfides under these conditions. Resistance to bulk corrosion is reflected in their recoveries: after H_2S exposure followed by recovery in pure H_2, a $Pd_{78}Ag_9Au_{13}$ ternary alloy membrane displayed the highest permeability of all the samples tested, including the $Pd_{91}Au_9$ binary alloy. Our results validate the strategy of using Au as a ternary component to improve the H_2S tolerance of high permeability PdAg.

2. Experimental

2.1. Membrane preparation

Membranes were deposited by sequential electroless plating of alloy components onto ZrO_2-modified, porous (0.1 μm grade), stainless steel 316L discs, 1.27 cm diameter × 2 mm thick. Before metal deposition, the discs were washed with an alkaline solution consisting of 0.12 M $Na_3PO_4 \cdot 12H_2O$, 0.6 M Na_2CO_3 and 1.12 M NaOH using the procedure reported by Ma and coworkers [23], and then treated in air for 12 h at 773 K. To avoid intermetallic diffusion between the stainless steel substrate and the alloy components, the supports were modified with ZrO_2 by a vacuum-assisted dip coating method [24]. Before the electroless plating step, the discs were activated. The sensitizing activation of the substrate was performed at room temperature, first in an acidic $SnCl_2$ (1 g/L) solution, and then in an acidic $PdCl_2$ solution (0.1 g/L). The sensitizing-activation process was repeated six times. Palladium, silver and gold were deposited by sequential electroless deposition using the bath compositions shown in Table 1. For the sample with the lower Ag content, palladium was deposited in two steps of 60 min each, followed by a short Ag deposition of 5 min. In the case of the sample with the higher Ag content, palladium was deposited in two steps of 60 min and 40 min each, followed by Ag deposition for 15 min. For both samples, the Au deposition on top of the Pd–Ag layers was performed for 20 min. For the PdAg sample, palladium was deposited in two steps of 60 min each, followed by a short Ag deposition of 5 min. The average deposition rates (Table 1) of Pd, Ag and Au were 1.8, 1.5 and 0.3, respectively. After the metal depositions, the samples were rinsed with water and dried at 393 K overnight. The two- and three-metal deposition cycle was repeated for both samples to achieve a target thickness of ~14 μm. The thickness of the metal layers was determined by the gravimetric method. The values estimated by this method were in good agreement with those determined from the SEM images.

Table 1
Chemical composition of Pd, Ag and Au electroless plating solutions, activation and plating conditions.

	Activation/pH modifier	Plating bath		
		Pd	Ag	Au
$SnCl_2$ (g/L)	1.0	–	–	–
$PdCl_2$ (g/L)	0.10	–	–	–
HCl (M)	1.0	–	–	–
Hydrazine (mM)		10	10	–
28–30% NH_4OH (M)	–	9.8	9.8	–
Na_2EDTA (g/L)	–	180	180	–
$PdCl_2$ (mM)	–	20.3	–	–
$AgNO_3$ (mM)	–	–	10	–
$Na_2S_2O_3 \cdot 5H_2O$ (mM)	–	–	–	150
Na_2SO_3 (mM)	–	–	–	170
$C_6H_8O_6$ (mM)	–	–	–	340
$AuCl_3 \cdot HCl \cdot 4H_2O$ (mM)	–	–	–	10.1
pH	–	11.5	11.5	11.0
Temperature (K)	–	323	323	333
Deposition rate (μm/h)		1.8	1.5	0.3

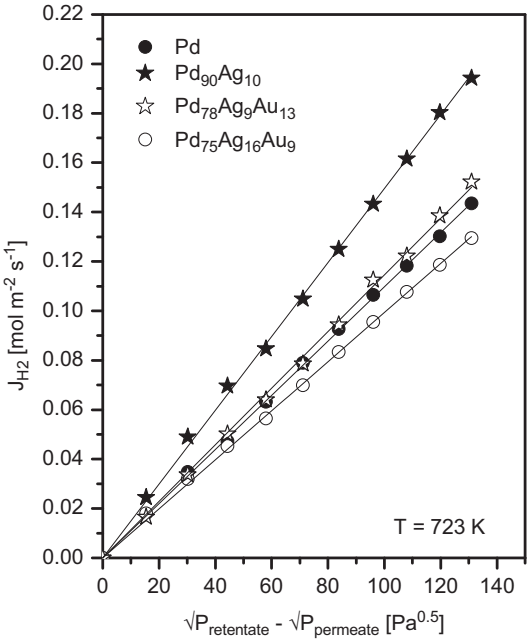

Fig. 1. Hydrogen flux through the membranes as a function of pressure difference at 723 K.

The ternary and $Pd_{90}Ag_{10}$ alloy membranes were annealed at 873 K in H_2 for 72 h to promote metallic inter-diffusion and alloy formation. The $Pd_{91}Au_9$ alloy was annealed at 773 K for 120 h. The samples were mounted in a disc permeation apparatus [19] and heated from room temperature to the annealing temperature at 0.5 K min^{-1} in flowing nitrogen.

2.2. Permeation measurement and H_2S treatment

Permeation experiments were conducted using a permeation apparatus described elsewhere [19]. Disc membrane samples were mounted in the apparatus, exposing a permeation area of 1.2 cm^2. The apparatus was covered by heating tapes and heated to the desired experimental temperatures. A thermocouple mounted beneath the disc was used to control the temperature during the experiments. High-purity H_2 and N_2 were used in all experiments; feed gas flow rates were set using calibrated mass-flow controllers. The Pd alloy layer was in contact with feed gases, while the permeate side was fed with N_2 as sweep gas during the heating and annealing procedure. No sweep gas flow was used on the permeate side during the single-gas permeation experiments. Pressure differences across the membranes were controlled by a closed-loop system with pressure sensor; the upstream pressure was varied whereas the downstream pressure was held constant at 100 kPa. The permeate flow rates were measured using bubble flowmeters at room temperature and pressure.

To evaluate their responses to H_2S, membranes were exposed to a 100 ppm H_2S/H_2 gas mixture at 673 K for 24 h at a transmembrane pressure of 50 kPa. After the H_2S exposure, the apparatus was fed with pure hydrogen at the same temperature and pressure. The hydrogen flux through the membrane was measured throughout both stages of the experiment. During these experiments no sweep gas was fed on the permeate side. Nitrogen was not detected at a transmembrane pressure of 200 kPa either before or after the H_2S treatments, showing that neither the thermal treatment nor the H_2S exposure had a detrimental effect on the selectivity.

2.3. Membrane materials characterization

2.3.1. X-ray diffraction

To confirm alloy formation and to identify possible sulfide corrosion products, the phase structure of the samples was determined by X-ray Diffraction. The XRD patterns of the films were obtained with an XD-D1 Shimadzu instrument, using Cu Kα (λ=1.542 Å) radiation at 30 kV and 40 mA. The scan rate was 1–2° min^{-1} in the range 2θ=15–90°.

2.3.2. Scanning electron microscopy, mapping and energy-dispersive X-ray analysis

Images of the outer surfaces and cross-sections of the samples were obtained using a JEOL scanning electron microscope, model JSM-35C, equipped with an energy dispersive analytical system (EDAX). The atomic compositions of the membranes, measured by EDS, were $Pd_{90}Ag_{10}$, $Pd_{91}Au_9$, $Pd_{78}Ag_9Au_{13}$ and $Pd_{75}Ag_{16}Au_9$.

3. Results and discussion

3.1. Hydrogen permeation properties

Fig. 1 shows the hydrogen flux measured across $Pd_{90}Ag_{10}$, both PdAgAu ternary alloys and a Pd reference membrane at 723 K in

Table 2
Hydrogen permeability of the Pd and Pd alloy membranes at several temperatures.

Temperature (K)	Permeability × 10^8 (mol m^{-1} s^{-1} $Pa^{-0.5}$)				
	$Pd_{91}Au_9$[a]	Pd	$Pd_{75}Ag_{16}Au_9$	$Pd_{78}Ag_9Au_{13}$	$Pd_{90}Ag_{10}$
623	–	0.91	1.03	1.07	1.34
648	–	1.06	1.10	1.19	1.49
673	0.99	1.21	1.18	1.34	1.65
698	–	1.37	1.27	1.49	1.84
723	1.30	1.53	1.38	1.63	2.08

[a] Reference [24].

Table 3
Summary of literature permeability results involving the effect of H_2S exposure to Pd and Pd alloy membranes at several temperatures.

Membrane (%)	Temperature (K)/time of exposure (h)	Permeability[a] (mol m^{-1} s^{-1} $Pa^{-0.5}$)	H_2S treatment	Experiment result upon H_2S exposure	Reference
Pd	593/120	8.0×10^{-9}	20 ppm H_2S/60% H_2–He	Bulk Pd_4S formation	Mundschau [7]
Pd	623/6	1.3×10^{-8}	1000 ppm H_2S/10% He–H_2	Bulk Pd_4S formation	O'Brien [15]
Pd	673/24	1.2×10^{-8}	100 ppm H_2S in H_2	Bulk Pd_4S formation	This work
$Pd_{75}Ag_{25}$	593/65	1.8×10^{-8}	10 ppm H_2S/80% H_2–He	Bulk Pd_4S and $Ag_5Pd_{10}S_5$ formation	Mundschau [7]
$Pd_{73}Ag_{27}$	623/48	1.9×10^{-8}	3.5 ppm H_2S in H_2	Dull and etched surface	McKinley [8]
$Pd_{90}Ag_{10}$	673/24	1.65×10^{-8}	100 ppm H_2S in H_2	Bulk Pd_4S formation	This work
$Pd_{74}Au_{26}$	623/6	5.1×10^{-9}	66,000 ppm H_2S in H_2	Maintains H_2 flux after H_2S treatment	McKinley [8]
$Pd_{88}Au_{12}$	673/100	1.0×10^{-8}	20 ppm H_2S/50%H_2/ 29%H_2O/19%CO_2/1%CO	High tolerance and selectivity	Gade [14]
$Pd_{94}Au_6$	673/80	1.1×10^{-8}		Pd_4S and $Pd_{2.8}S$ formation	Gade [14]
$Pd_{91}Au_9$	673–723	$1.1–1.5 \times 10^{-8}$	–	–	Tarditi [24]
$Pd_{91}Au_9$	673–723	$1.0–1.2 \times 10^{-8}$	–	–	Tarditi [24]
$Pd_{94.5}Au_{5.5}$	773/4	4.7×10^{-9}	54.8 ppm H_2S in H_2	65% H_2 flux recovery	Ma [13]
$Pd_{91}Au_9$	673/24	1.1×10^{-8}	100 ppm H_2S in H_2	80% H_2 flux recovery and maintains select	This work
$Pd_{87}Au_7Pt_6$	673/100	1.0×10^{-8}	20 ppm H_2S/50%H_2/ 29%H_2O/19%CO_2/1%CO	Pd_4S formation and loss of selectivity	Coulter [22]
$Pd_{89}Au_5Pt_6$	673/82	6.1×10^{-9}		Maintains H_2 flux and selectivity after H_2S	Coulter [22]
$Pd_{67}Ag_8Cu_{25}$	673/1	5.4×10^{-9}	–	–	Tarditi [19]
$Pd_{85}Ag_{11}Cu_4$	673/1	7.8×10^{-9}	20 ppm H_2S/90% H_2–N_2	Bulk Pd_4S formation	Bredesen [21]
$Pd_{69}Ag_{27}Y_4$	673/1	1.1×10^{-8}	20 ppm H_2S/90% H_2–N_2	Sulfur surface contamination	Bredesen [21]
$Pd_{76}Ag_{21}Mo_3$	673/1	5.0×10^{-9}	20 ppm H_2S/90% H_2–N_2	Sulfur surface contamination	Bredesen [21]
$Pd_{75}Ag_{22}Au_3$	673/1	8.5×10^{-9}	20 ppm H_2S/90% H_2–N_2	Maintains H_2 flux after H_2S treatment	Bredesen [21]
$Pd_{74}Ag_{14}Au_{12}$	623/30	–	1000 ppm H_2S in H_2	No bulk sulfides were detected	Braun [20]
$Pd_{78}Ag_9Au_{13}$	673/24	1.3×10^{-8}	100 ppm H_2S in H_2	80% H_2 flux recovery and high selectivity	This work
$Pd_{75}Ag_{16}Au_9$	673/24	1.2×10^{-8}	100 ppm H_2S in H_2	65% H_2 flux recovery and high selectivity	This work

[a] Permeability measured in pure H_2 before the H_2S treatment.

the absence of H_2S as a function of $\Delta P^{0.5}$. Linear relationships between flux and $\Delta P^{0.5}$ confirm that H-atom diffusion is the limiting step of hydrogen transport rates for all samples [25]. $Pd_{90}Ag_{10}$, with the steepest slope, displays the highest permeability among these samples at 723 K. Permeabilities of the same samples, and a $Pd_{91}Au_9$ membrane, measured at temperatures from 623 to 723 K are displayed in Table 2. Permeability varied within the sample set as $Pd_{90}Ag_{10} > Pd_{78}Ag_9Au_{13} > Pd \sim Pd_{75}Ag_{16}Au_9 > Pd_{91}Au_9$. In other words, both ternary membranes displayed lower permeabilities than the $Pd_{90}Ag_{10}$ alloy membrane, but higher permeabilities than the $Pd_{91}Au_9$ membrane over this temperature range.

Hydrogen permeabilities of related binary and ternary Pd alloys, and their responses to H_2S, have been reported by a number of researchers. Table 3 is a summary of relevant examples selected from the literature. In binary alloys with Pd, Ag has been widely observed to increase permeability, whereas Au usually suppresses it [8,13,14,24]. However, the H_2 permeation measurements performed in this work revealed that the ternary alloy membrane with less Ag and higher Au content ($Pd_{78}Ag_9Au_{13}$) showed higher permeability than the $Pd_{75}Ag_{16}Au_9$ alloy membrane. These results show that the behavior of H_2 permeation in ternary alloys membranes is more complex than in binary alloys, and it is necessary to evaluate the H_2 transport through PdAgAu alloy membranes in a wide range of Ag and Au compositions to allow a better discussion of the influence of metal composition on permeability.

In recent years, measurements of hydrogen transport through ternary alloy membranes have been reported [18,20–22]. Uemiya and coworkers [18] synthesized a $Pd_{69}Ag_{30}Ru_1$ alloy membrane by electroless codeposition and reported that its permeability was three times higher than that of pure Pd. Bredesen and coworkers [21] studied the addition of a number of minor ternary components on PdAg alloys, $\sim Pd_{75}Ag_{20}X_5$ (X=Au, Mo, Cu, Y) [21]; in all cases, they observed lower H_2 permeabilities than either pure Pd or the PdAg binary. We previously [20] reported results for a PdAgAu alloy, which displayed a permeability slightly higher than that of pure Pd. Coulter et al.[22] reported self-supported 25 μm thick $Pd_{86}Au_6Pt_6$(target

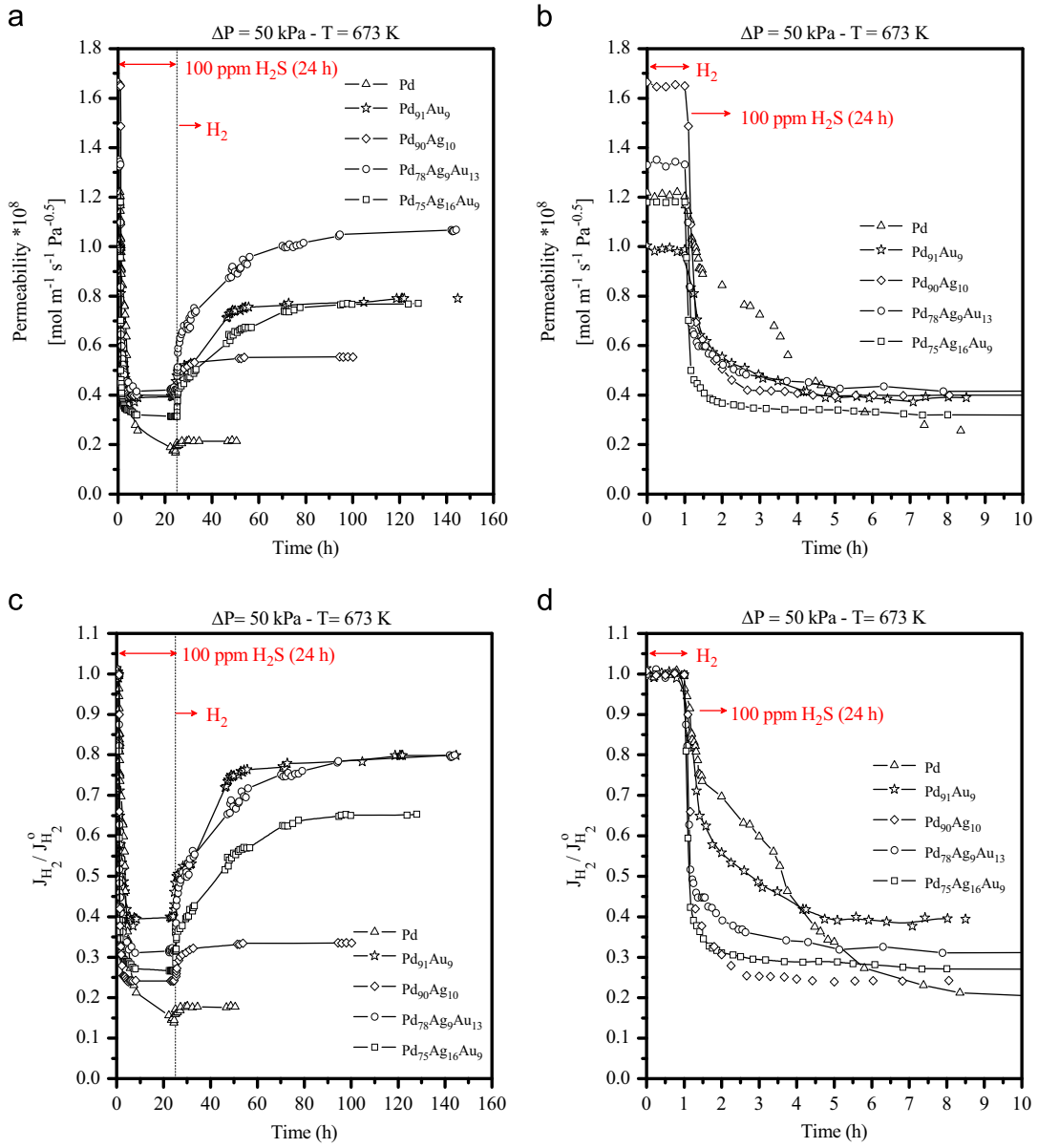

Fig. 2. Permeability (a, b), and relative H_2 (c, d) flux (J/J^o) during the H_2S fed through the membranes as a function of time. H_2S treatment conditions: T=673 K, [H_2S]= 100 ppm, time=24 h, ΔP=50 kPa.

composition) alloy membranes with H_2 permeabilities ($0.12–1.41 \times 10^{-8}$ mol m^{-1} s^{-1} $Pa^{-0.5}$) that depended on the sputtering conditions. Because the published reports span a range of ternary components, composition of components and preparation methods, drawing general conclusions about designing a ternary alloy with high permeability is difficult.

3.2. H_2S treatment: hydrogen inhibition transport and flux recovery

At the end of the pure hydrogen permeation experiments, 100 ppm H_2S was added to the feed gas to assess the inhibition of H_2 transport by H_2S. Then, after 24 h of H_2S exposure at 673 K, the feed gas was changed back to pure hydrogen to study H_2 flux recovery. Fig. 2a shows measured permeabilities as function of time on stream during H_2S exposure and during subsequent recovery in H_2. All membranes experienced a large decrease in H_2 permeability immediately on introduction of H_2S. The primary cause of the rapid decrease is site blocking by adsorbed H_2S [15,17,21]. The permeability of pure Pd, and to a lesser extent $Pd_{90}Ag_{10}$, continued to decline throughout the H_2S exposure period, evidence of growth of a low permeability bulk (microns-thick) sulfide scale [4,15]. At the end of the 24 h H_2S exposure, the membranes displayed a range of permeability decline: $Pd_{91}Au_9$ (60% decrease) $< Pd_{78}Ag_9Au_{13} < Pd_{75}Ag_{16}Au_9 < Pd_{90}Ag_{10} <$ Pd (85% decrease).

The membranes also displayed a range of recovery responses on removal of H_2S from the feed gas. Pd and the $Pd_{90}Ag_{10}$ binary membrane experienced only very small recoveries immediately on removal of H_2S, with modest (PdAg) or no (Pd) incremental improvement over time. This behavior is also characteristic of formation of stable, low permeability bulk (microns-thick) sulfide layers at the membrane surfaces. Consistent with this observation, the XRD patterns of these samples after the permeation experiment, shown in Fig. 3, reveal the presence of Pd_4S [26] and, in the case of $Pd_{90}Ag_{10}$, $Ag_5Pd_{10}S_5$ sulfides [27]. The higher permeation recovery observed for $Pd_{90}Ag_{10}$ in comparison with the Pd membrane may be related to a thinner sulfide scale, less bulk sulfide contamination detected by EDS.

In contrast to the Pd and $Pd_{90}Ag_{10}$ membranes, the PdAgAu ternaries and the $Pd_{91}Au_9$ binary exhibited a rapid partial recovery of H_2 permeability, which is likely related to desorption of H_2S that had been blocking surface sites. These samples then experienced additional recovery at a slower rate that stabilized asymptotically after ~40 h, but none recovered all of its original pure H_2 permeability. This pattern suggests partial reversal of surface poisoning by strongly adsorbed S and/or 'two-dimensional' (nanometers thick) sulfide layers may be related to different metal–sulfur bond interactions at the surface. Through theoretical calculations, Alfonso [28] showed a weaker Pd–S bond interaction as the sulfur coverage was increased; the repulsive force between sulfur atoms with increasing sulfur coverage may be responsible for this phenomenon. The XRD patterns of the PdAgAu ternaries and $Pd_{91}Au_9$ (Fig. 3) are also consistent with surface poisoning; these samples displayed features of only the parent fcc solid alloy solution, with no evidence of bulk sulfide formation. After 80 h in pure H_2, the membranes recovered to different extents: $Pd_{91}Au_9 \approx Pd_{78}Ag_9Au_{13}$ (80% of initial H_2 permeability) $> Pd_{75}Ag_{16}Au_9$ (65%) $> Pd_{90}Ag_{10}$ (33%) $>$ Pd (17%). Fig. 2b summarizes the relative flux (where J_{H_2} is the H_2 flux at a given time and $J^o_{H_2}$ is the H_2 flux measured in pure H_2 before H_2S exposure for the same membrane) of all the membranes tested.

SEM/EDS characterization of the morphology and composition of the H_2S-exposed membranes confirm the link between bulk sulfide formation and nonrecoverable H_2S deactivation. Fig. 4 shows SEM top-views of the membranes at two magnification scales (a–j) and Fig. 5 shows their EDS spectra. As expected, the Pd membrane showed a large number of pinholes on the surface, characteristic of bulk Pd_4S formation [5,7,9,20]. The sulfur content of the pure Pd membrane was 3.5%, highest among the sample set. While pinholes were not observed in the $Pd_{90}Ag_{10}$ membrane, EDS analysis revealed a high sulfur content (1.8% S). Unlike Pd and $Pd_{90}Ag_{10}$, none of the Au-containing alloys displayed detectable S. The $Pd_{75}Ag_{16}Au_9$ alloy showed a dendritic morphology, which can be related to the higher Ag content [20,29,30].

To assess the composition homogeneity through the ternary alloy membranes, both PdAgAu membranes were characterized by EDS in a cross-sectional region. Fig. 6 shows the cross-sectional micrographs and corresponding Pd, Ag and Au % atomic composition profiles of the PdAgAu membranes after the annealing and the H_2–H_2S/H_2 permeation measurements. Cross-sectional EDS characterization revealed a uniform composition for the three metal-containing alloy;

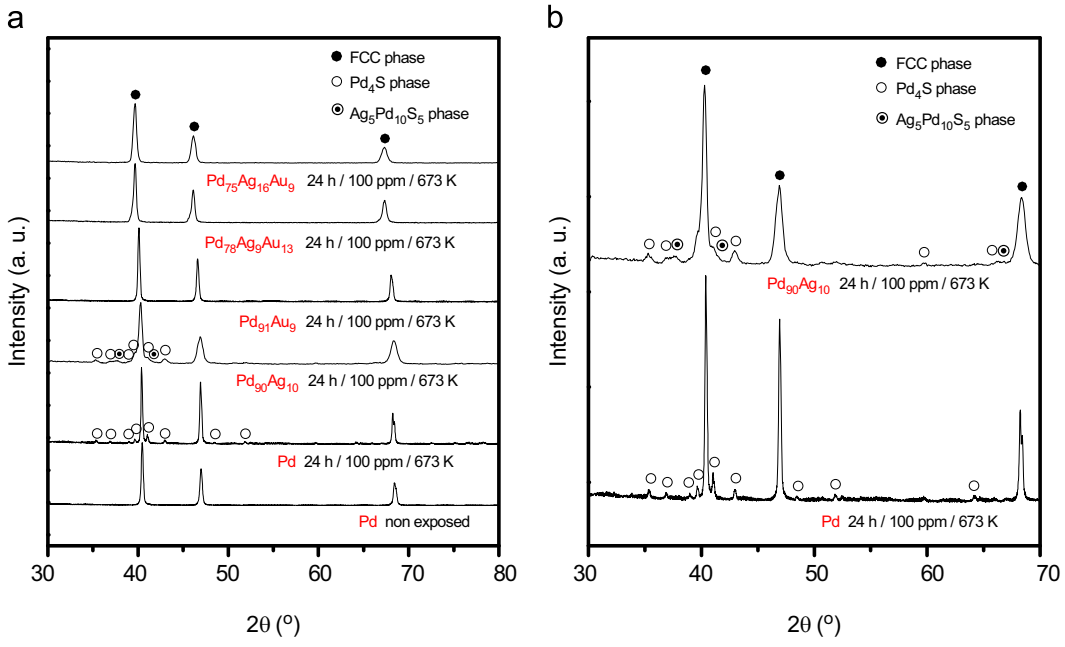

Fig. 3. X-ray diffraction patterns of the membranes after H_2S exposure. Annealing conditions of $Pd_{90}Ag_{10}$ and ternary samples: 72 h at 873 K in H_2. Annealing conditions of PdAu sample: 120 h at 773 K in H_2. H_2S treatment conditions: T=673 K, [H_2S]=100 ppm, time=24 h, ΔP=50 kPa.

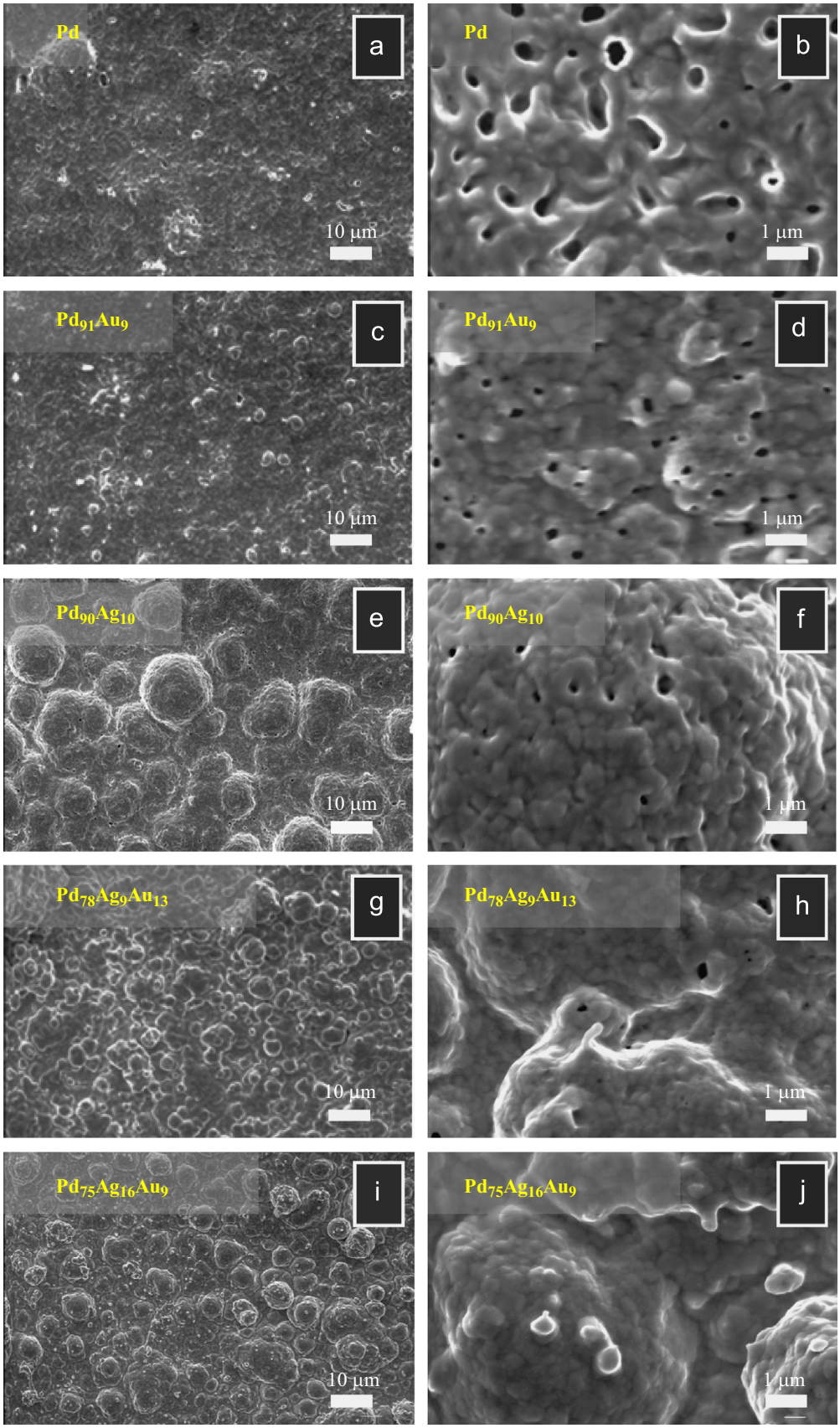

Fig. 4. SEM top view of Pd (a, b), $Pd_{91}Au_9$ (c, d), $Pd_{90}Ag_{10}$ (e, f), $Pd_{78}Ag_9Au_{13}$ (g, h), $Pd_{75}Ag_{16}Au_9$ (i, j) membranes after H_2S exposure. H_2S treatment conditions: $T=673$ K, $[H_2S]=100$ ppm, time=24 h, $\Delta P=50$ kPa.

this result shows that the annealing process was suitable to achieve a ternary alloy with a uniform composition in the 14 μm-thick film.

Our observations of low permeability in the presence of H_2S with relatively little recovery for both Pd and $Pd_{90}Ag_{10}$ are consistent with other reports of sulfur corrosion and permeability loss for Pd and PdAg membranes on exposure to even low H_2S concentrations [9,10]. Likewise, our results for $Pd_{91}Au_9$ are consistent with other published reports of PdAuH_2S response. For example, Chen and Ma reported that $Pd_{95.5}Au_{4.5}$ lost 85% of its permeability after 4 h in 54.8 ppm H_2S at 673 K [13]; our sample lost less permeability on exposure to 100 ppm H_2S for 24 h, likely because of its higher Au content. On removal of H_2S, $Pd_{95.5}Au_{4.5}$ alloy recovered ~65% of its original permeability. These authors also reported the H_2 relative flux of the $Pd_{95.5}Au_{4.5}$ alloy membrane in pure H_2 after H_2S exposure; while a 4 h exposed membrane required more than 60 h to achieve 65% of its original permeability, a 24 h exposed membrane required more than 150 h. Note that 75 h were needed for our $Pd_{91}Au_9$ membrane to achieve 80% of its original permeability. Like our $Pd_{91}Au_9$, XRD analysis of the postexposure membrane samples revealed no evidence of bulk sulfide formation [13].

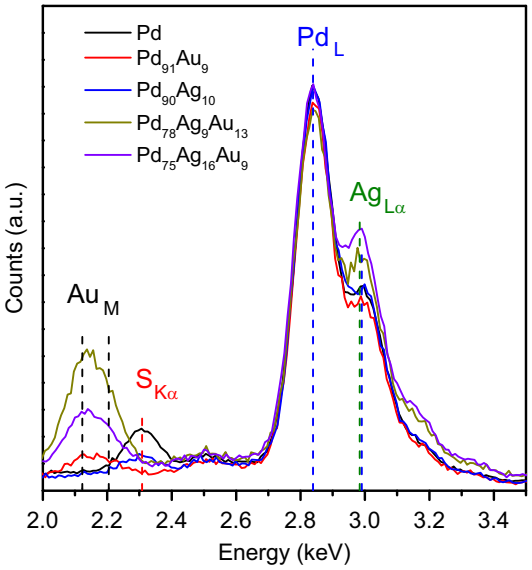

Fig. 5. Energy-dispersive X-ray spectra of Pd, $Pd_{91}Au_9$, $Pd_{90}Ag_{10}$, $Pd_{78}Ag_9Au_{13}$ and $Pd_{75}Ag_{16}Au_9$ membranes after H_2S exposure. H_2S treatment conditions: T=673 K, [H_2S]=100 ppm, time=24 h, ΔP=50 kPa.

Gade et al. [14] evaluated the permeability of $Pd_{94}Au_6$ and $Pd_{89}Au_{11}$ alloys in synthetic water–gas shift (WGS) streams containing H_2S. Addition of 20 ppm H_2S to the WGS mixture reduced the permeability of $Pd_{94}Au_6$ and $Pd_{89}Au_{11}$ by 50% and 40%, respectively. After H_2S/WGS testing, XRD analysis of $Pd_{94}Au_6$ revealed formation of Pd_4S and $Pd_{2.8}S$, suggesting that at least part of the flux reduction could be related to the scale formation [14]. This result differs from those of Chen and Ma [13], who observed no bulk formation on exposure of a similar membrane to H_2S/H_2 mixtures (no WGS components). This difference suggests that the presence of the WGS components facilitates sulfide corrosion of PdAu alloys.

Less common are studies of ternary alloy responses to H_2S. We previously reported that $Pd_{83}Ag_2Au_{15}$ and $Pd_{74}Ag_{14}Au_{12}$ alloys, similar to those described here, did not form bulk sulfides on exposure to 1000 ppm H_2S/H_2 at 623 K for 30 h, conditions that readily convert pure Pd to Pd_4S [20]. Coulter et al. [22] evaluated a $Pd_{89}Au_5Pt_6$ membrane; in the presence of a WGS mixture, addition of 20 ppm H_2S reduced the $Pd_{89}Au_5Pt_6$ permeability by ~20% after 82 h of exposure at 673 K. These authors also reported that the membrane $Pd_{89}Au_5Pt_6$ displayed full recovery of H_2 flux when

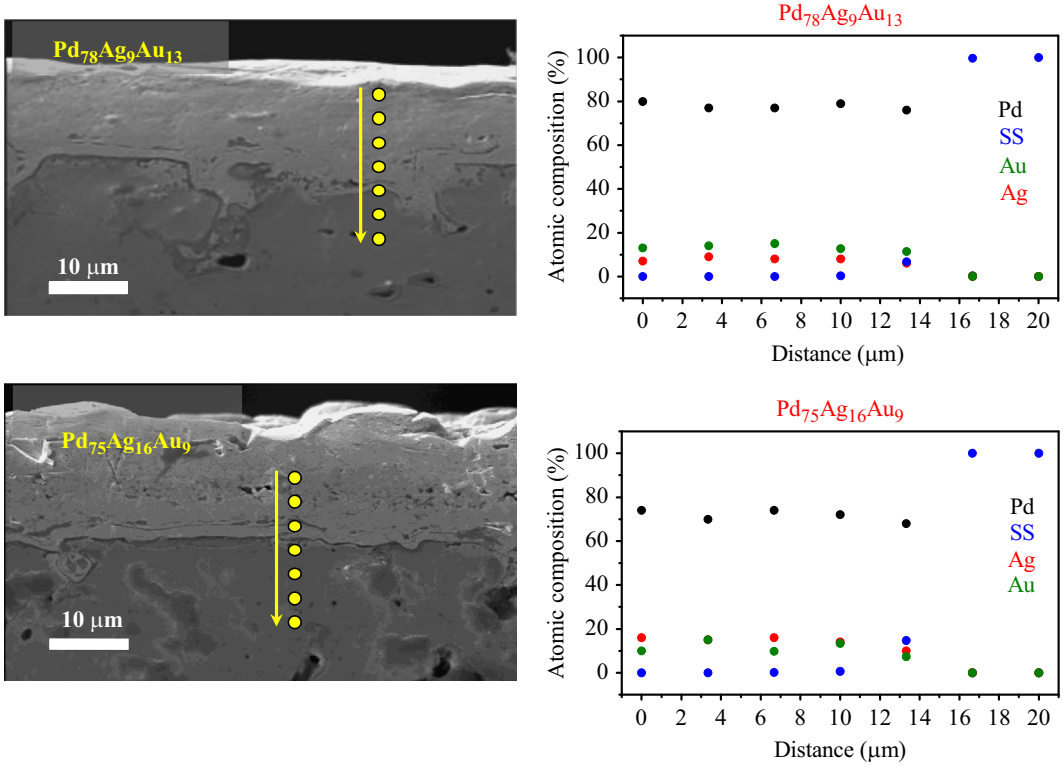

Fig. 6. Cross-sectional SEM and EDS characterization of $Pd_{78}Ag_9Au_{13}$ and $Pd_{75}Ag_{16}Au_9$ membranes after H_2S exposure. H_2S treatment conditions: T=673 K, [H_2S]=100 ppm, time=24 h, ΔP=50 kPa.

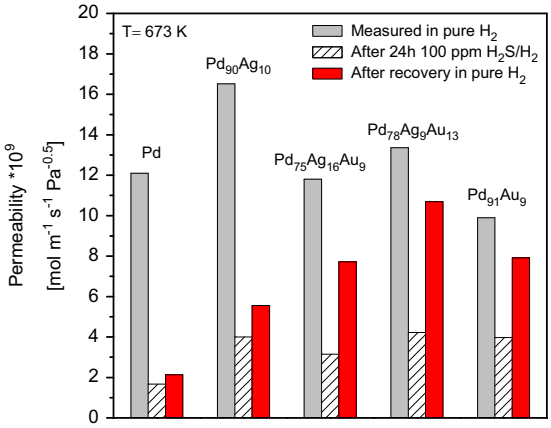

Fig. 7. H_2 permeability through the membranes measured in pure H_2, after 24 h of H_2S treatment and after steady flux recovery. H_2S treatment conditions: T=673 K, [H_2S]=100 ppm, time=24 h, ΔP=50 kPa. H_2 flux recovery conditions: T=673 K, 100% H_2, ΔP=50 kPa.

exposed to H_2S in a WGS mixture. However, a ternary alloy membrane with a similar composition, $Pd_{87}Au_7Pt_6$, exhibited deterioration of selectivity and Pd_4S formation (by glancing-incidence X-ray diffraction) after 100 h of exposure at 673 K in the same gas mixture. In agreement with our results, Bredesen et al. [21] reported that a $Pd_{75}Ag_{22}Au_3$ membrane prepared by magnetron sputtering showed an improved performance in the presence of 20 ppm H_2S/H_2 mixtures at 723 K in comparison with a $Pd_{77}Ag_{23}$ membrane (and no formation of a bulk sulfide).

Fig. 7 summarizes initial (before H_2S exposure) H_2 permeability, permeability after 24 h in 100 ppm H_2S, and permeability after recovery in H_2 for the five membranes examined in this work. As described earlier, alloying of Pd with 10 at% Ag increases the H_2 permeability of pure Pd. But, as shown in Fig. 2, $Pd_{90}Ag_{10}$ is susceptible to S poisoning and exhibits low flux recovery. $Pd_{91}Au_9$, in contrast, recovers to 80% of its pre-H_2S exposure permeability, but its initial permeability is relatively low (compared to pure Pd). Improved S tolerance of the PdAu binary can be traced to its resistance to form a bulk sulfide. A significant finding of this work is that a ternary alloy, $Pd_{78}Ag_9Au_{13}$, can combine Ag ability to increase flux with Au sulfur tolerance to deliver a membrane that exhibits higher permeability than pure Pd and resists formation of bulk sulfides on H_2S exposure. Thus, our results illustrate the effectiveness of ternary alloying as a strategy to improve the performance of Pd-based membranes across multiple performance dimensions.

4. Conclusions

$Pd_{78}Ag_9Au_{13}$ and $Pd_{75}Ag_{16}Au_9$ alloy separation membranes, prepared by electroless deposition technique, display (pure) H_2 permeabilities that are comparable with or slightly higher than those of pure Pd. The ternary alloys display H_2 permeabilities that are significantly higher than a reference $Pd_{91}Au_9$ membrane but lower than a reference $Pd_{90}Ag_{10}$ membrane. On exposure to 100 ppm H_2S/H_2 at 673 K for 24 h, the ternary membranes, the binary references and pure Pd all experienced significant permeability reductions, ranging from 60% loss for $Pd_{91}Au_9$ to 85% loss for pure Pd. After a recovery period in pure H_2, Au-containing alloys regained much of their original permeabilities; $Pd_{91}Au_9$ and $Pd_{78}Ag_9Au_{13}$ membranes recovered to ~80% of initial H_2 permeability. Notably, with its higher pure H_2 permeability, $Pd_{78}Ag_9Au_{13}$ displayed the highest absolute H_2 permeability after recovery. Recovery by the Au-containing alloys is related to Au ability to prevent formation of thick, stable sulfide corrosion layers on the membrane surfaces. Our results show that addition of Au to the high-permeability PdAg binary delivers a PdAgAu ternary that minimizes the permanent H_2 flux loss associated with H_2S exposure by preventing formation of thick stable sulfides.

Acknowledgments

The authors wish to acknowledge the financial support received from UNL and ANPCyT. Elsa Grimaldi is thanked for the English language editing and Fabio Fontanarrosa is hereby thanked for the SEM images acquisition.

References

[1] S. Uemiya, W. Kato, A. Uyama, M. Kajiwara, T. Kojima, E. Kikuchi, Separation of hydrogen from gas mixtures using supported platinum-group metal membranes, Sep. Purif. Technol. 22–23 (2001) 309–317.
[2] N.W. Ockwig, T.M. Nenoff, Membranes for hydrogen separation, Chem. Rev. 107 (2007) 4078–4110.
[3] S.N. Paglieri, J.D. Way, Innovations in palladium membrane research, Sep. Purif. Rev. 31 (2002) 1–169.
[4] C.P. O'Brien, A.J. Gellman, B.D. Morreale, J.B. Miller, The hydrogen permeability of Pd_4S, J. Membr. Sci. 371 (2011) 263–267.
[5] B.D. Morreale, B.H. Howard, O. Iyoha, R.M. Enick, C. Ling, D.S. Sholl, Experimental and computational prediction of the hydrogen transport properties of Pd_4S, Ind. Eng. Chem. Res. 46 (2007) 6313–6319.
[6] T.A. Peters, T. Kaleta, M. Stange, R. Bredesen, Development of thin binary and ternary Pd-based alloy membranes for use in hydrogen production, J. Membr. Sci. 383 (2011) 124–134.
[7] M.V. Mundschau, X. Xie, C.R. Evenson, A.F. Sammells, Dense inorganic membranes for production of hydrogen from methane and coal with carbon dioxide sequestration, Catal. Today 118 (2006) 12–23.
[8] D.L. McKinley, Metal alloy for hydrogen separation and purification. US Patent 3,350,845, 1967.
[9] B.D. Morreale, The Influence of H_2S on Palladium and Palladium–Copper Alloy Membranes, Chemical Engineering, Doctor of Philosophy, University of Pittsburgh, 2006.
[10] P. Kamakoti, B.D. Morreale, M.V. Ciocco, B.H. Howard, R.P. Killmeyer, A. V. Cugini, D.S. Scholl, Prediction of hydrogen flux through sulfur-tolerant binary alloy membranes, Science 307 (2005) 569–573.
[11] O. Iyoha, R. Enick, R. Killmeyer, B. Howard, M. Ciocco, B. Morreale, H_2 production from simulated coal syngas containing H_2S in multi-tubular Pd and 80 wt% Pd–20 wt% Cu membrane reactors at 1173 K, J. Membr. Sci. 306 (2007) 103–115.
[12] O. Iyoha, R. Enick, R. Killmeyer, B. Morreale, The influence of hydrogen sulfide to-hydrogen partial pressure ratio on the sulfidization of Pd and 70 mol% Pd–Cu membranes, J. Membr. Sci. 305 (2007) 77–92.
[13] C.-H. Chen, Y.H. Ma, The effect of H_2S on the performance of Pd and Pd/Au composite membrane, J. Membr. Sci. 362 (2010) 535–544.
[14] S.K. Gade, S.J. DeVoss, K.E. Coulter, S.N. Paglieri, G.O. Alptekin, J.D. Way, Palladium–gold membranes in mixed gas streams with hydrogen sulfide: effect of alloy content and fabrication technique, J. Membr. Sci. 378 (2011) 35–41.
[15] C.P. O'Brien, B.H. Howard, J.B. Miller, B.D. Morreale, A.J. Gellman, Inhibition of hydrogen transport through Pd and $Pd_{47}Cu_{53}$ membranes by H_2S at 350 °C, J. Membr. Sci. 349 (2010) 380–384.
[16] A. Kulprathipanja, G. Alptekin, J. Falconer, J.D. Way, Pd and Pd–Cu membranes: inhibition of H_2 permeation by H_2S, J. Membr. Sci. 254 (2005) 49–62.
[17] C.P. O'Brien, J.B. Miller, B.D. Morreale, A.J. Gellman, The Kinetics of H_2-D_2 Exchange over PdCu Surfaces in the Presence of H_2S, J. Phys. Chem. C116 (2012) 17657–17667.
[18] L. Wang, R. Yoshiie, S. Uemiya, Fabrication of novel Pd–Ag–Ru/Al_2O_3 ternary alloy composite membrane with remarkably enhanced H_2 permeability, J. Membr. Sci. 306 (2007) 1–7.
[19] A.M. Tarditi, F. Braun, L.M. Cornaglia, Novel PdAgCu ternary alloy: hydrogen permeation and surface properties, Appl. Surf. Sci. 257 (2011) 6626–6635.
[20] F. Braun, J.B. Miller, A.J. Gellman, A.M. Tarditi, B. Fleutot, P. Kondratyuk, L. M. Cornaglia, PdAgAu alloy with high resistance to corrosion by H_2S, Int. J. Hydrogen Energy 37 (2012) 18547–18555.
[21] T.A. Peters, T. Kaleta, M. Stange, R. Bredesen, Development of ternary Pd–Ag–*TM* alloy membranes with improved sulphur tolerance, J. Membr. Sci. 429 (2013) 448–458.
[22] K.E. Coulter, J.D. Way, S.K. Gade, S. Chaudhari, G.O. Alptekin, S.J. DeVoss, Sulfur tolerant PdAu and PdAuPt alloy hydrogen separation membranes, J. Membr. Sci. 405–406 (2012) 11–19.
[23] Y.H. Ma, B.C. Akis, M.E. Ayturk, F. Guazzone, E.E. Enqwall, I.P. Mardilovich, Characterization of intermetallic diffusion barrier and alloy formation for Pd/Cu and Pd/Ag porous stainless steel composite membranes, Ind. Eng. Chem. Res. 43 (2004) 2936–2945.
[24] A. Tarditi, C. Gerboni, L. Cornaglia, PdAu membranes supported on top of vacuum-assisted ZrO_2-modified porous stainless steel substrates, J. Membr. Sci. 369 (2011) 267–276.

[25] S. Yun, S.T. Oyama, Correlations in palladium membranes for hydrogen separation: a review, J. Membr. Sci. 3375 (2011) 28–45.
[26] JCPDS International Centre for Diffraction Data. Card # 73-1387 (1962).
[27] JCPDS International Centre for Diffraction Data. Card # 27-1156 (1971).
[28] D.R. Alfonso, First-principles study of sulfur overlayers on Pd(1 11) surface, Surf. Sci. 596 (2005) 229–241.
[29] M.E. Ayturk, E.A. Payzant, S.A. Speakman, Y.H. Ma, Isothermal nucleation and growth kinetics of Pd/Ag alloy phase via in situ time-resolved high-temperature X-ray diffraction (HTXRD) analysis, J. Membr. Sci. 316 (2008) 97–111.
[30] M.L. Bosko, E.A. Lombardo, L.M. Cornaglia, The effect of electroless plating time on the morphology, alloy formation and H_2 transport properties of PdAg composite membranes, Int. J. Hydrogen Energy 36 (2011) 4068–4078.